Journal of ELECTRONIC MATERIALS, Vol. 32, No. 8, 2003 *Special Issue Paper*

Gas-Cluster Ion-Beam Smoothing of Chemo-Mechanical-Polish Processed GaSb(100) Substrates

L.P. ALLEN,[1,6] T.G. TETREAULT,[1] C. SANTEUFEMIO,[1] X. LI,[2] W.D. GOODHUE,[2] D. BLISS,[3] M. TABAT,[1] K.S. JONES,[4] G. DALLAS,[5] D. BAKKEN,[5] and C. SUNG[2]

1.—Epion Corporation, Billerica, MA 01821. 2.—Photonics Center, University of Massachusetts at Lowell, Lowell, MA 01854. 3.—Air Force Research Laboratory/SNHC, Hanscom AFB 01731. 4.—Department of Materials Science, University of Florida, Gainesville, FL 32611. 5.—Galaxy Compound Semiconductor, Spokane, WA 99206. 6.—E-mail: lallen@attbi.com

Gas-cluster ion-beam (GCIB) processing of surfaces provides individual atoms within an accelerated gas cluster (~1,500 atoms per cluster), an energy approximately equal to the individual bond energy of the target surface atoms. The gas-cluster beam is thus capable of providing smoothing and etching of the extreme surface of numerous semiconductors, metals, insulators, and magnetic materials. For semiconductor material systems, the gas-cluster processing effect on the surface and subsurface material is of critical interest for device and circuitry application integrity. In the case of III-V GaSb, chemo-mechanical or touch polishing is the final step in the semiconductor-wafer manufacturing process, often leaving scratches of various depths or damage on the polished surface. In this paper, we report the GCIB etching and smoothing of chemical-mechanical polished GaSb(100) wafers. Using a dual-energy, dual gas-cluster source process, $\sim$100 nm of material was removed from a GaSb(100) surface. Atomic-force microscopy (AFM) imaging and power spectral-density (PSD) analysis shows significant decrease in the post-GCIB root-mean-square (Rms) roughness and peak-to-valley measurements for the material systems. X-ray rocking-curve analysis has shown a 24-arcsec reduction in the full-width at half-maximum (FWHM) of the (111) x-ray diffraction peak of GaSb. High-resolution transmission-electron microscopy (HRTEM) shows the crystallinity of the subsurface of the pre- and post-GCIB surfaces to be consistent, following the 1×10^{16} ions/cm^2 total-fluence processes, with dislocation density for both pre- and post-GCIB cases below the HRTEM resolution limit. X-ray photoelectron spectroscopy (XPS) indicates a strong Ga 3p electron binding-energy intensity for gallium-oxide formation on the GaSb surface with the use of an oxygen GCIB process. Analysis of the Ga 3p electron binding-energy peaks in the XPS data in conjunction with HRTEM indicates a higher Ga or GaSb content in the near-surface layer (less stoichiometric-oxide presence) with use of a CF_4/O_2 GCIB process. The same peak analysis indicates that the surface gallium-oxide state is nearly unchanged, except in thickness, with the use of an O_2-GCIB second step. The material results suggest that GCIB provides a viable method of chemo-mechanical polish (CMP) damage removal on group III-V material for further device processing.

Key words: Surface smoothing, gas-cluster ion beam (GCIB), surface modification, GaSb, CMP

(Received September 10, 2002; accepted March 10, 2003)

INTRODUCTION

Recent technology trends require atomically smooth and uniform surface layers without surface or subsurface damage. During conventional smoothing on semiconductor substrates, residual damage and nonuniformity may result from a chemo-mechanical polish (CMP). The removal of CMP or touch-polish damage from the substrate surface is of primary interest in many materials applications. Gas-cluster ion-beam (GCIB) processing of material surfaces is a recent technology that has been successfully used to etch, atomically smooth, and provide uniform substrate materials.[1–5] This paper addresses the use of GCIB technology for damage removal on GaSb using a dual-energy, dual-gas species, shallow etching, and a smoothing process. The GaSb (100), purchased from University Wafers (South Boston, MA),[6] was examined by atomic-force microscopy (AFM) imaging and power spectral-density (PSD) analysis, x-ray photoelectron spectroscopy (XPS), x-ray rocking-curve analysis, and high-resolution transmission-electron microscopy (HRTEM) for analysis of material quality and surface morphology as well as the surface-oxidation states. This study shows that a higher energy GCIB process was successfully used to remove ~100 nm of material beyond the damage depth. A second process step used a low-energy process for GCIB smoothing. A change in the low-energy gas source from a fluorinated species to an oxygen-molecule GCIB did not significantly affect the root-mean-square (Rms) surface roughness or average surface roughness (Ra) but did increase the relative peak intensity of the gallium-oxide, electron-binding energy. The surface etching, smoothing, and oxidation of the GaSb films are presented and discussed.

The GCIB processing is based on the use of gas-cluster ions, each consisting of a few thousand atoms or molecules of gaseous material. The kinetics of an atomic-cluster ion impinging on a surface is quite different from that of an ion-implanted atom into a target. A 1,000-atom gas cluster accelerated through 10 kV yields an average, individual atom energy of 10 eV as the cluster impacts the surface. This average energy is very large compared with the typical binding energy (<0.1 eV/argon atom) of the clusters, and hence, the impacts are highly inelastic.[7]

The general GCIB apparatus schematic is shown in Fig. 1. Gas-cluster formation is achieved through supersonic gas expansion from a high-pressure source into a vacuum via a small orifice or nozzle. The adiabatic expansion reduces the relative velocity of the gas atoms and condensation into clusters is favored. The nozzle, a key component to gas-cluster beam formation, determines the cluster size and beam-flow pattern and will serve to remove some heat from the atomic collision process, thus assisting in the gas-cluster formation. Gas clusters with mean sizes ranging from 500 atoms to 10,000 atoms can be held together by van der Waals forces. A small aperture, or skimmer, collects the primary jet core of gas clusters. The forward-directed neutral clusters are ionized by impact of electrons emitted and accelerated from a filament (Fig. 1). This forms positive-ion gas clusters of nominally one electron charge per cluster. The ionized clusters are extracted and accelerated (typically from 2 kV to 25 kV) using a series of electrodes. Electrostatic lenses are used to focus the cluster ions, and monomers are filtered out

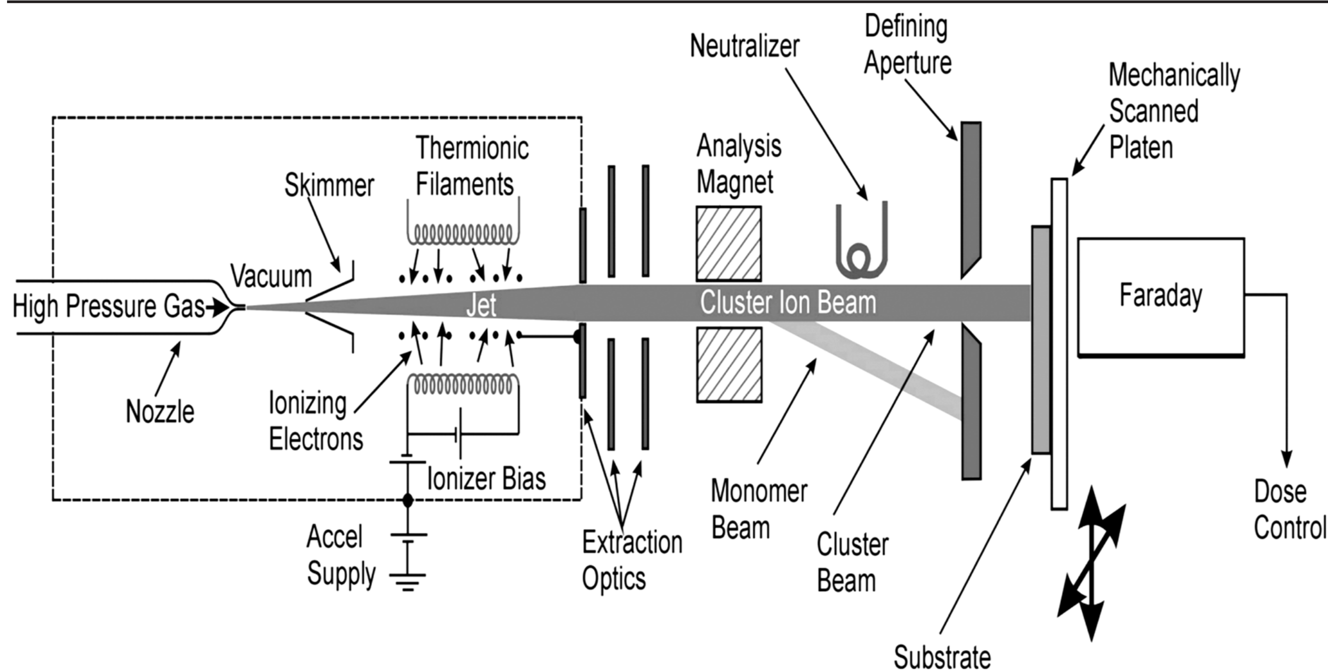

Fig. 1. A GCIB apparatus schematic.[7]

through the use of a transverse magnetic field. Ion fluence is measured by a Faraday cup and, in the system shown later, the sample is mechanically scanned for complete wafer coverage.

Examination of surface roughness both prior to and after the GCIB impingement process has shown that numerous material types can be smoothed using Ar and other source-gas clusters.[8–11] The CMP or touch-polish damage or scratch reduction, however, requires a shallow etching as well as a smoothing process be applied to the substrate surface. The surface atoms must be etched away to a minimum depth equivalent to the bottom of the deepest scratch or more. While surface scratches may be reduced or eliminated, the subsurface material strain associated with deep CMP scratches may still be present for hundreds of angstroms within the subsurface. Thus, the GCIB process may be used to etch below the scratch depths to further alleviate subsurface material strain.

EXPERIMENT: GAS-CLUSTER ION-BEAM ETCHING AND SMOOTHING

In this study, the dual-energy, dual-gas-species GCIB process for the GaSb surface consisted of a 10-kV CF_4/O_2 etch step followed by a 3-kV O_2 smoothing step for a total charge fluence of 1.5×10^{16} ions/cm^2.

The as-received CMP surfaces and post-GCIB surfaces of GaSb(100) were examined by a Digital Instruments Nanoscope III atomic-force microscope with Si tips used in the tapping mode. The surface roughness (Rms and Ra) and peak-to-valley measurements (Rmax) were quantified at both 1 μm $\times$ 1 μm and 10 μm $\times$ 10 μm scan sizes. In addition to the AFM images, the PSD comparison for the pre-GCIB and post-GCIB surfaces was obtained. The PSD represents the spatial-frequency content of the surface roughness.[12] The differences in the surface-feature frequencies were converted to a power-spectrum density distribution by multiplying the square of the frequency-variation strength by the volume over which the various surface roughnesses are being sampled (μm^3). When plotted against the length scale over which the fluctuations were detected, ranging from 0.001 μm to 10 μm, the result is a curve that represents actual distributions of the surface-feature shape frequencies as observed through the Fourier transformation process.

A Philips (Philips Electronic Instruments Corp., Mahwah, NJ) high-resolution, x-ray rocking-curve instrument with four-circle scanning capability (Cu K_α) was used to determine the pre-GCIB and post-GCIB full-width at half-maximum (FWHM) for the (400) and (111) diffraction peaks of GaSb (100). As the width of the rocking curve is a direct measure of the range of strain present in the irradiated area of the crystal, the FWHM of a rocking-curve diffraction peak is, essentially, a measurement of the quality of the irradiated-crystal area.

The HRTEM cross sections of the GaSb substrates were examined using a JEOL (Japan Electron Optics Ltd., Tokyo) 2010 HRTEM with a field-emission gun. Standard gluing, dimpling, and ion-milling cross-sectional TEM sample-preparation techniques were employed. Images were formed by orientation of the sample such that the transmitted beam was parallel to the (100) plane and ⟨110⟩ direction of the GaSb-lattice surface. An objective aperture that allows transmission of 13 beams was used to form the phase-contrast images.

The approximate chemical composition of the pre-GCIB and post-GCIB GaSb surface was also examined through XPS. The surface-oxidation state is an important consideration for epitaxial layer growth on GaSb. For this research, the estimated thickness of the oxide surface as well as the relative stoichiometry were examined to determine the best surface for post-GCIB molecular-beam-epitaxy (MBE) material deposition and device applications. The XPS analysis was performed on a PHI Model 5600 Multi-Technique system comprised of a Model 10-360 electron-energy analyzer (SCA) with an Omni-Focus III input lens to the analyzer. Monochromatic Al K_α x-rays were used at 1,486.6 eV. Energy calibration for the system was verified relative to Au 4f 7/2 at 84.0 eV, Ag 3d5/2 at 368.25 eV, and Cu 2p3/2 at 932.67 eV. Any minor surface charging was corrected by shifting the adventitious C 1s peak to 285.0 eV. The GCIB surfaces were examined at two different takeoff angles, 20° and 75°, relative to the surface plane, with the 20° data shown in this paper. In addition to these angles, the CMP control surface was also examined at 45°. In this way, relative changes in composition with depth could be investigated without the uncertainties involved with sputter-depth profiling. Survey spectra were taken as well as high-resolution acquisitions on the Ga 3p, Sb 3d, and C 1s peak positions. Peak fitting and quantification of the data were performed using *CasaXPS* from Casa Software, Ltd. (Devon, UK).[13]

RESULTS

The AFM images for the as-received and post-GCIB surfaces of GaSb are shown in Fig. 2a–d. The tilted images are shown in identical x-y-z scale and contrast. For the multiple area scans of the 1 μm $\times$ 1 μm images, the average surface Rmax was reduced from 12.9 nm to 1.8 nm, and the average Ra was reduced from 1.1 nm to 0.17 nm. For the multiple area scans of the 10 μm $\times$ 10 μm images, the average surface Rmax was reduced from 28.6 nm to 2.7 nm, and the average Ra was reduced from 0.82 nm to 0.19 nm. The shallow surface scratches produced by the CMP process were no longer visible in the AFM images. The PSD comparison for the 100-μm^2 AFM images is shown in Fig. 2e. Over the 10-μm wavelength scale, the PSD comparison shows that the intensity was significantly reduced at all surface-feature wavelengths. The 0.1-μm feature

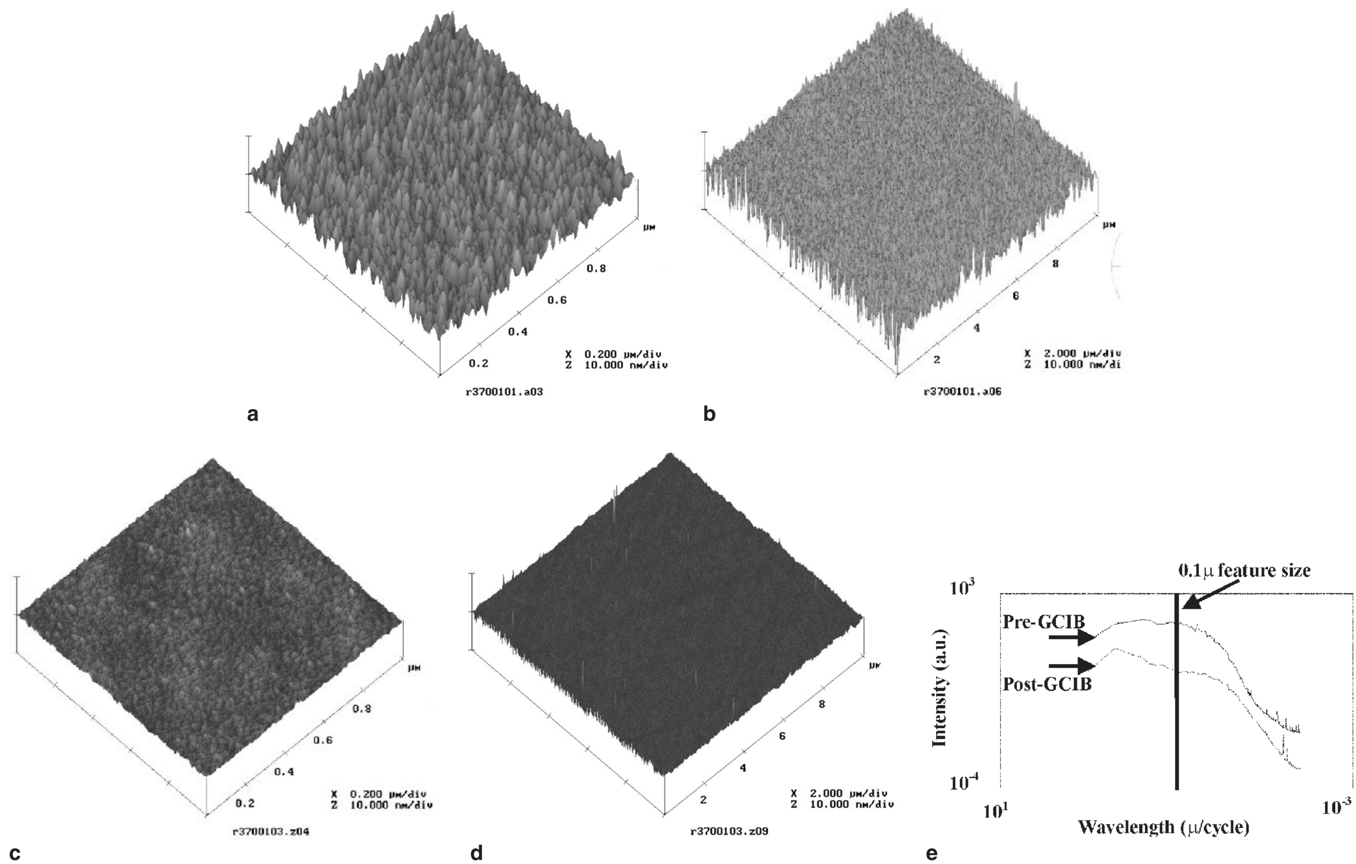

Fig. 2. (a) The AFM image (1 μm × 1 μm) of the as-received GaSb surface. The z range = 132 Å, Rms = 13.7 Å, and Ra = 10.9 Å for the lightly scratched GaSb surface. (b) The AFM image (10 μm × 10 μm) of the as-received GaSb surface. The z range = 268 Å, Rms = 10.5 Å, and Ra = 8.2 Å for the lightly scratched GaSb surface. (c) The AFM image (1 μm × 1 μm) of the post-GCIB GaSb surface. The z range = 28.7 Å, Rms = 2.5 Å, and Ra = 1.9 Å. Surface damage was significantly reduced after the dual-energy, dual-species GCIB process. (d) The AFM image (10 μm × 10 μm) of the post-GCIB GaSb surface. The z range = 75 Å, Rms = 3.0 Å, and Ra = 2.4 Å. Surface damage was significantly reduced after the dual-energy, dual-species GCIB process. (e) The PSD comparison of pre-GCIB and post-GCIB surface-feature intensity as a function of wavelength. The PSD comparison shows that all surface-feature wavelengths were reduced in intensity.

size for the pre- and post-GCIB processed GaSb is indicated in the PSD curve comparison.

The x-ray rocking-curve data are shown in Fig. 3 for the pre-GCIB and post-GCIB surface and subsurface material. Figure 3a (pre-GCIB) and b (post-GCIB) shows the GaSb FWHM for the (400) diffraction peak. The FWHM remained the same for that Bragg angle-diffraction peak with a slight (0.01) degree shift in the peak center after GCIB processing. Figure 3c (pre-GCIB) and d (post-GCIB) show the FWHM of the GaSb (111) diffraction peak. The (111) close-packed planes are more sensitive to material strain, with a lattice-constant strain decrease indicated by the decrease in the FWHM. For the post-GCIB GaSb surface, the FWHM was reduced by 24 arcsec and exhibited a slight shift in the peak center position by 0.01°. All x-ray rocking-curve counts per second reflect the same amount of time per total scan.

The HRTEM images for the pre-GCIB and post-GCIB GaSb surface and subsurface are shown in Fig. 4. Figure 4a is an image of the as-received material cross section and shows the undulating oxide coverage of the GaSb surface. The image suggests a total native-oxide surface coverage but with undulations in thickness. These undulating regions along the GaSb surface are observed in a thickness range from 0 Å to 20 Å. The HRTEM image of the post-GCIB GaSb material for the CF_4/O_2-GCIB dual-energy (10 kV followed by 3 kV, total dose 1×10^{16} ions/cm^2) process is shown in Fig. 4b. There, the noncrystalline surface layer is shown to be much thicker (~125 Å), but still undulating in thickness. Figure 4c shows the GaSb surface cross section after the dual-energy, dual-gas-species (10-kV CF_4/O_2, 3-kV O_2, total dose 1.5×10^{16} ions/cm^2) GCIB process. The surface oxide is shown to range from 20 Å to 40 Å, also in an undulating pattern. The image indicates that the dual-energy, dual-gas-species GCIB process did not induce subsurface dislocations or produce a subsurface amorphous layer. However, the images indicate that the undefined oxide-surface layer created by either GCIB process did continue the undulating thickness pattern encountered with the as-received GaSb surface. The total fluence of 1.5×10^{16} ions/cm^2 has ~2,000 atoms associated with each charge measured by the Faraday cup. The increased thickness of the undulating surface oxide

Fig. 3. (a) The x-ray rocking curve of the (400) diffraction peak for pre-GCIB GaSb. The FWHM is 16 arcsec at a peak position of 30.6815°. (b) The x-ray rocking curve of the (400) diffraction peak for post-GCIB GaSb. The FWHM remained at 16 arcsec with a slightly shifted peak position of 30.6963°. (c) The x-ray rocking curve of the (111) diffraction peak for pre-GCIB GaSb. The FWHM is 76 arcsec at a peak position of 12.3967°. (d) The x-ray rocking curve of the (111) diffraction peak for post-GCIB GaSb. The FWHM is reduced to 52 arcsec at a slightly shifted peak position of 12.3850°.

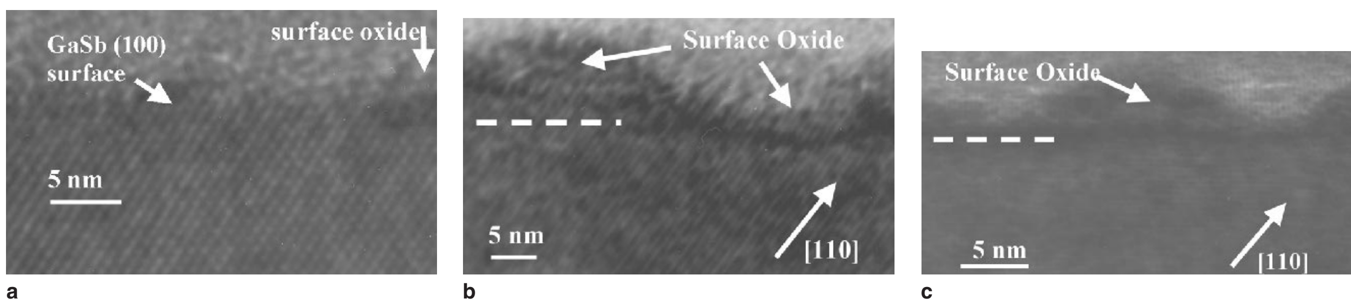

Fig. 4. (a) The HRTEM cross-section image of the pre-GCIB (as-received) GaSb(100). (b) The HRTEM cross-section image of the post-GCIB (dual-energy [10-kV, 3-kV] CF_4/O_2) process. (c) The HRTEM cross-section image of the dual-energy [10-kV, 3-kV], dual-gas-species process with oxygen GCIB as the final step.

after GCIB processing may be due to the stochastic overlay of the individual GCIB-impact craters[7,14] or from the growth of a GCIB oxide along the initial, sinusoidal type of thickness variation.

The surface oxides formed by GCIB processing have been examined by spectroscopic ellipsometry and XPS. With use of a final O_2-GCIB process step (such as in this study) on material that is able to react with oxygen, the post-GCIB material typically forms a thicker (more stoichiometric) oxide surface.[7,14] The XPS analysis of the Ga 3p peak is shown in Fig. 5 for the pre- and post-GCIB GaSb surface. Careful deconvolution of the peaks indicates the relative strength of the gallium-oxide signal versus the Ga- or GaSb-metal signal on the material surface in the pre- and post-GCIB condition.

One complication involved with achieving an accurate quantification of the surface composition of

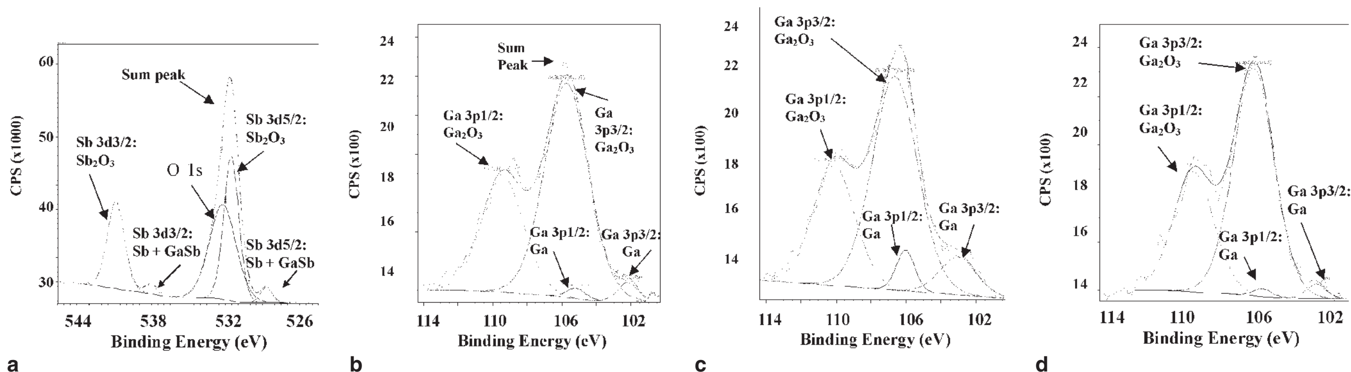

Fig. 5. (a) The XPS analysis of the Sb 3d electron binding-energy intensities for the unprocessed, CMP-finished GaSb(100) taken at 75° takeoff relative to the surface plane. (b) The XPS analysis of the Ga 3p electron binding-energy intensities for the unprocessed, CMP-finished GaSb(100). (c) The XPS analysis of the Ga 3p electron binding-energy intensities for the dual-energy GCIB-processed GaSb(100). (d) XPS analysis of the Ga 3p electron binding-energy intensities for the dual-energy, dual-gas-species GCIB-processed GaSb(100).

these samples, especially in terms of oxide analysis, is that the oxygen 1s electron binding-energy peak position in the XPS spectrum is directly overlapped by the chemically shifted, Sb 3d5/2 peak from antimony oxide. As a result, independent quantification of the oxygen content of various GaSb surface treatments is difficult. This makes a reliable quantification of the oxide stoichiometry problematic. In this study, to deconvolute the relative contribution of oxygen in the peak envelope at 532 eV, the Sb 3d3/2 peak was specifically examined relative to the Sb 3d5/2 peak as is shown in Fig. 5a. As the O 1s peak overlaps with the Sb 3d5/2 peak, an examination of the oxidation state of the Sb 3d3/2 peak allows for a quantification of the peak envelope that contains both the O 1s binding-energy intensity as well as the Sb 3d5/2 binding-energy intensity. Given the same sensitivity factors, the quantification of antimony oxide based upon the analysis of the Sb 3d3/2 peak should be identical to the analysis based upon the Sb 3d5/2 peak. The remaining integral area of the 532 eV peak envelope results from the O 1s binding-energy intensity.

A similar ratio analysis for the Ga 3p3/2 and Ga 3p1/2 binding-energy intensity was also performed. Figure 5b shows the as-received GaSb-surface XPS for the Ga 3p3/2 and Ga 3p1/2 electron binding-energy peaks. Figure 5c shows the same peaks after a CF_4/O_2-GCIB dual-energy (10 kV then 3 kV, total dose 1×10^{16} ions/cm^2) process. Figure 5d shows the same peaks after the dual-energy, dual-gas-species (10-kV CF_4/O_2 followed by 3-kV O_2, total dose 1.5×10^{16} ions/cm^2) GCIB process. The XPS clearly shows an increase in the metallic (Ga or GaSb) concentration in the surface layer relative to the oxide with use of the CF_4/O_2-GCIB dual-energy process. For the dual-energy, dual-gas-species process, the surface-oxidation state is nearly identical to that of the as-received GaSb substrate. Table I lists the values by percentage of the Ga metal versus the Ga_2O_3 concentration in the near-surface layer as analyzed by XPS. Although somewhat more complicated to evaluate, the results are important for understanding the nature of the oxidized-GaSb surface and the total amount of oxygen in the surface state.

Table I. Ga 3p Electron Binding-Energy Information

GaSb Surface	%Ga Metal	%Ga_2O_3
Unprocessed GaSb	3.7	96.3
Dual-energy GCIB process: 10-kV CF_4/O_2 and 3-kV CF_4/O_2	12.7	87.3
Dual-energy, dual-gas GCIB process: 10-kV CF_4/O_2, followed by 3-kV O_2	2.9	97.1

DISCUSSION

The PSD comparison of Fig. 2e shows a significant intensity reduction in the submicron surface-feature anomaly size up to ~3-μm feature size of the spectrum. The comparison of the pre-GCIB and post-GCIB PSD curves represents the surface-roughness data over the specified range of frequency and describes the overall effect of the wafer smoothing on the GaSb surface. A key aspect of the PSD is that the graph provides a measure of the surface roughness across a spatial-frequency range, preventing an inadvertently incorrect assessment of the surface-roughness changes based upon individual-area, quantitative AFM measurements. For the GCIB manufacturing process employed, improvement in the surface roughness of the GaSb features was observed across the entire spectrum.

The HRTEM analysis shows a native oxide on the surface of the pre-GCIB GaSb with the substoichiometric surface oxide appreciably increased in the post-GCIB GaSb. The undulating pattern remains for the GaSb surface-oxide growth when using either the fluoride or the pure oxygen-molecule GCIB for the final step of the dual-energy, dual-species process. Of interest for further optoelectronic-device processing is the evidence from the HRTEM cross

section that the surface under the oxide is confirmed to be smoother, consistent with the AFM results. In the process of material removal through GCIB etching away the shallow surface scratches, the subsurface was not damaged. No dislocation formation is observed in the HRTEM cross sections as shown in the consistent lattice imaging. The use of the HRTEM in conjunction with the XPS data was quite useful in determining the thickness versus the oxygen concentration for the surface layer of the post-GCIB processed GaSb.

A semiconductor oxide layer is usually used for passivation or insulation and serves as a protective coating for wafer handling prior to epi or device processing. Published studies on GaSb oxides are relatively few[15–17] but important in light of the requirement for GaSb-surface oxides to clean or desorb prior to epitaxy or optoelectronic-device processing. The results of the XPS analysis suggest that the preferred surface-oxidation state is Ga_2O_3, and the oxidized Sb is minimal in comparison. This is most likely due to the higher vapor pressure of the Sb. Such information is important for subsequent MBE or device-process work, as the somewhat passivating Ga_2O_3 is preferred for a controlled, subsequent in-situ high-vacuum desorption. The comparison between the glancing angle-incidence measurements indicate that the use of an oxygen-GCIB finishing step ensures the preference for a near-stoichiometric gallium oxide over an antimony oxide state.

CONCLUSIONS

The CMP shallow surface damage of GaSb were etched and smoothed by a dual-energy, dual-gas-species GCIB process. The AFM studies show a significant decrease in the surface roughness and shallow scratch visibility after ~100 nm of GaSb material removal, with the average Ra measurement decreasing to <0.2 nm. The PSD of the material surface shows that a decrease in intensity for a large frequency range across the surface occurs with the GCIB process. The HRTEM images support the improvement in surface smoothness and show a thicker material-oxide formation on the surface of the GaSb after GCIB processing that is consistent with other GCIB surface studies. The XPS results suggest a more pronounced, Ga_2O_3 relative-peak intensity, which may prove beneficial for subsequent MBE deposition on the surface layer. The HRTEM images did not show subsurface damage resulting from the GCIB process.

ACKNOWLEDGEMENTS

The authors enjoyed valuable discussions pertaining to this work with Wes Skinner, David Fenner, Mike Mack, and Allen Kirkpatrick of Epion Corporation. The GCIB SOI development support of the USAF under Contract No. F33615-00-C-5404 is sincerely appreciated. The GaSb wafer support from Contract No. DAAH01-03-CR018 is gratefully acknowledged.

REFERENCES

1. I. Yamada, J. Matsuo, N. Toyoda, and A. Kirkpatrick, *Mater. Sci. Eng. R* 34, 231 (2001).
2. D.B. Fenner, R.P. Torti, L.P. Allen, N. Toyoda, A.R. Kirkpatrick, J.A. Greer, V. DiFilippo, and J. Hautala, *Mater. Res. Soc. Symp. Proc.* 585, 27 (2000).
3. I. Yamada and J. Matsuo, *Mater. Res. Soc. Symp. Proc.* 396, 149 (1996).
4. L.P. Allen, D.B. Fenner, V. DiFilippo, C. Santeufemio, E. Degenkolb, W. Brooks, M. Mack, and J. Hautala, *J. Electron. Mater.* 30, 829 (2001).
5. D.B. Fenner, V. DiFilippo, T.G. Tetreault, J.K. Hirvonen, and L.C. Feldman, *Proc. SPIE* 4468, 17 (2001).
6. University Wafer, South Boston, MA, http://www.UniversityWafer.com
7. L.P. Allen, Z. Insepov, C. Santeufemio, D.B. Fenner, W. Brooks, K.S. Jones, and I. Yamada, *J. Appl. Phys.* 92, 3671 (2002).
8. D.B. Fenner, J. Hautala, L.P. Allen, T.G. Tetreault, A. Al-Jibouri, J.I. Budnick, and K.S. Jones, *J. Vac. Sci. Technol. A* 19, 1207 (2001).
9. M.S. Hatzistergos, H. Efstathiadis, E. Lifshin, A.E. Kaloyeros, J.L. Reeves, V. Selvamanickam, L.P. Allen, and R. MacCrimmon, *J. Supercond.* (in print).
10. L.P.Allen, S. Caliendo, N. Hofmeester, E. Harrington, M. Walsh, M. Tabat, T.G. Tetreault, E. Degenkolb, C. Santeufemio, and W. Skinner, *Proc. IEEE Int. SOI Conf.,* Williamsburg, VA, 7–11 October 2002.
11. Z. Insepov, M. Sosnowski, and I. Yamada, *Nucl. Instrum. Meth. B* 127/128, 269 (1997).
12. E. Marx, I.J. Malik, Y.E. Strausser, T. Bristow, N. Poduje, and J.C. Stover, *J. Vac. Sci. Technol. B* 20, 31 (2002).
13. *CasaXPS* is a product of Casa Software Ltd., Teignmouth, Devon, UK.
14. L.P. Allen, D.B. Fenner, C. Santeufemio, W. Brooks, J. Hautala, and Y. Shao, *SPIE Int. Symp. Optical Sci. Technol.* 4806, 225 (2002).
15. N. Kitamura, T. Kikuchi, M. Kakeh, and T. Wada, *Jpn. J. Appl. Phys.* 23, 1534 (1984).
16. N. Kitamura and S. Okada, *Mater. Lett.* 21, 111 (1994).
17. N. Kitamura, *Trans. IEICE* E 73, 198 (1990).